Desalination and Water Treatment
www.deswater.com

doi: 10.5004/dwt.2019.24246

158 (2019) 301–308
August

Preparation of poly[3-(methacryloylamino) propyl] trimethylammonium chloride coated mesh for oil–water separation

Jeng-Yi Wu, Chao-Wei Huang, Ping-Szu Tsai*

Department of Chemical and Materials Engineering, National Kaohsiung University of Science and Technology, No. 415, Jiangong Road, Sanmin District, Kaohsiung City 80778, Taiwan, R.O.C., Tel. +886-7-3814526 Ext: 15139; emails: charles1@nkust.edu.tw (P.-S. Tsai), supershatman@gmail.com (J.-Y. Wu), Tel. +886-7-3814526 Ext: 15135; email: huangcw@nkust.edu.tw (C.-W. Huang)

Received 21 December 2018; Accepted 8 April 2019

ABSTRACT

This study aims to prepare a polymer-coated mesh which could achieve good oil–water separation efficiency with an antibacterial property. These polymers were synthesized by the polymerization process of [3-(methacryloylamino) propyl] trimethylammonium chloride (MAPTAC). The hydrolysis resistance and the swelling ratio of the polymers were also examined in order to choose a suitable oil–water separation material. The prepared meshes showed not only high oil–water separation efficiency (>99%) with high permeate flux (up to 4,308 L h^{-1} m^{-2}), but also a good antibacterial property. In addition, the oil–water separation efficiencies exceed 99% even under various severe conditions, such as acidic (1 M HCl), alkaline (1 M NaOH), and salty (8 wt.% NaCl) solutions. The excellent durability of the polymer-coated mesh shows the fact that it is a facile and promising filtration mesh for oil–water separation.

Keywords: [3-(Methacryloylamino) propyl] trimethylammonium chloride; Oil–water separation; Polymer-coated mesh; Antibacterial property; Durability

1. Introduction

Since oil spill accidents, as well as oil pollution from industrial and restaurant wastewater, happened frequently [1–4], the separation of oily wastewater has been noticed worldwide due to the environmental issue. Current oil–water separation technologies such as mechanical separation, oil adsorption, filtration, air flotation and coagulation [5–10] could treat some accidents and pollutants; however, these technologies were usually inefficient and have high operating cost [11]. Gravity-driven membrane technology is regarded as a potential filtration for oil–water separation due to its low cost, energy-sufficient, and chemical-free process, but its low permeate flux would be the major limitations to utilization [12–14]. Therefore, porous filtration meshes or membranes have attracted attention due to simplicity and high permeate flux. The oil–water separation membranes inspired by fish scales have been widely adopted to solve the problem [15–18] due to its anti-oil properties and underwater superoleophobicity. Nevertheless, the complication of multiplying bacteria on membranes was gradually revealed in recent years [19–23].

Multiplying bacteria is a serious and complex problem for oil–water separation. Oily wastewater often contains acids, alkalis and high concentration of salts, even bacteria such as *Escherichia coli*. The presence of bacteria has adverse effects on the membrane separation process [24], for example, increasing membrane filtration resistance [25] and required energy [26], leading to the deterioration of the membranes' performance [27] and service life [26]. In order to prevent the multiplying bacteria problems, an antimicrobial surface containing inorganic antibacterial materials was coated on the oil–water separation membranes, such as graphene oxide-SiO_2 hybrids [28], graphene oxide [29], and copper [30]. With regard to these methods, there is thereby unavoidable release from the antibacterial membranes,

* Corresponding author.

such as inorganic powders or metal ions. It would cause secondary pollution and restrict their service life. On the contrary, organic antibacterial materials such as quaternary ammonium compounds [31], chitosan [32], halamine compounds [33], and antibacterial enzymes or peptides [34,35] have the ability to form covalent bond with the matrix of the membranes; hence, the release problems for antibacterial materials could be avoided.

Among these organic antibacterial materials, quaternary ammonium antimicrobials especially play an important role in the development of antibacterial surfaces [36]. They have high antibacterial efficiency against a wide range of microorganisms, such as gram-positive, gram-negative bacteria, fungi, and certain types of viruses [37,38]. Yao et al. produced the poly(D,L-lactide) (PDLLA) fibrous membranes modified with quaternary ammonium moieties and the membranes showed above 99.99% antibacterial efficiency against gram-positive (*Staphylococcus aureus*) and gram-negative (*Escherichia coli*) bacteria. It was proposed that there is a strong interaction between the positive charges of quaternary ammonium groups and the negative cell walls of bacteria, leading to its good antibacterial ability [39]. Inspired by the concept of the PDLLA modification, two kinds of quaternary ammonium polymers, [2-(methacryloyloxy)ethyl) trimethylammonium chloride (MAETAC) and [3-(methacryloylamino) propyl] trimethylammonium chloride (MAPTAC), were synthesized to verify their oil–water separation efficiency in this study. The effects of various proportions of monomer and a crosslinking agent for polymerization were also discussed. In addition, the hydrolysis resistance and the swelling ratio of these synthesized polymers were examined as well. We prepared the oil–water separation meshes by coating these antibacterial polymers on the stainless steel meshes during polymerization. Their oil–water separation efficiency, antibacterial ability, permeate flux, and durability were discussed below.

2. Material and methods

2.1. Materials

In order to synthesize the polymers, [2-(methacryloyloxy) ethyl] trimethylammonium chloride solution (MAETAC, 80%) and [3-(methacryloylamino) propyl]trimethylammonium chloride solution (MAPTAC, 50%) were chosen as the monomers; N,N,methylenebisacrylamide (MBA, 99%) was the crosslinking agent; ammonium persulfate (APS, ≥95%) was the initiator. All chemicals mentioned above were obtained from Sigma-Aldrich (St. Louis, MO, USA). Stainless steel meshes (pore size 4, 13, 26, 45, 63, 75, and 150 μm) were purchased from Yung Sheng Wire Co., Ltd., (Taichung, Taiwan). The vegetable oil of oil–water mixture was used as the pollutant source obtained from Standard Food Corporation (Taipei, Taiwan).

2.2. Preparation of polymer solutions

In order to clarify the properties of the synthesized polymers, we prepared five different types of polymers to characterize their hydrolysis resistance and swelling ratio. For the polymerization process, monomers (20 g of MAETAC or MAPTAC), a crosslinking agent (0.1, 0.2, 0.3, and 0.5 g of MBA), and an initiator (0.5 g of APS) were solved in deionized water by stirring for 1 h. The specimen ID and its raw materials of polymers were shown in Table 1. The polymer solutions were used as the coating material for preparing the oil–water separation meshes.

2.3. Hydrolysis resistance test

Initially, the polymer solutions would be heated to remove the solvent in an oven at 85°C for 180 min to get the dry polymers. Since the hydrolysis resistance test was carried out in a closed reactor, we added 1 g of the dry polymer into 100 mL of 0.5 M HCl solution in a vessel. The reaction temperature would be maintained at 50°C in 12–92 h. After that, the vessel was cooled in 20 min under sealed conditions. Sequentially, the solid residue was collected from the solution by filtration, washed by distilled water until the pH = 7, and then dried at 80°C in a vacuum oven until reaching a constant final mass. The dried solid residue was ground into powder by a mortar, and then we dissolved 0.5 g of the powder in 50 mL of a mixed solvent (2-methylphenol and chloroform with mass ratio = 7:3) at a temperature of 90°C for 45 min. Besides, phenolphthalein was added as an indicator for the potentiometric titration with standard ethanolic NaOH solution. When the titration was carried out, the endpoint was determined by the observation of a faint pink color [40]. Therefore, the end carboxyl-group concentration, $C_{(COOH)}$ (mol g^{-1}), could be obtained by the following equation:

$$C_{(COOH)} = \frac{\left(V_A - V_B\right) \times C_A}{m} \tag{1}$$

V_A (mL) was the volume of ethanolic NaOH which was consumed by sample solution, V_B (mL) was the volume of ethanolic NaOH which was consumed by blank solution, C_A (mol L^{-1}) was the concentration of ethanolic NaOH, and m (g) was the weight of the solid residual powder.

2.4. Swelling ratio test

Swelling ratio test is a simple method to characterize the networks of polymers. It is competed by the free energy of mixing and elastic retractive force, so it is also regarded as an index for polymer structures with different levels of crosslinking. In this study, we used the tea-bag weight method

Table 1
Specimen ID and its raw materials of the polymers

Specimen ID	Monomer		Crosslinker	Initiator
	MAETAC (g)	MAPTAC (g)	MBA (g)	APS (g)
PT-1	0	20	0.1	0.5
PT-2	0	20	0.2	0.5
PT-3	0	20	0.3	0.5
PT-4	0	20	0.5	0.5
TE-1	20	0	0.1	0.5

[41] to evaluate the swelling ratio. First, 0.500 g of dry polymers was enclosed in a tea bag (40 mm × 50 mm) and placed into 100 mL of water. The polymers started to swell while they were steeped in water. The samples were weighed several times in intervals until their weight reached equilibrium. Sequentially, the swelling ratio could be calculated by using the following formula:

$$Q = \frac{m_1 - m_0}{m_0} \times 100\% \quad (2)$$

where Q is the swelling ratio (g/g), and m_1 and m_0 denote the weight of the swollen and dry polymer, respectively.

2.5. Preparation of polymer-coated oil–water separation mesh

The as-prepared polymer solutions were deposited on the cleaned stainless steel (pore size 4, 13, 26, 45, 63, 75, and 150 μm) by the dip-coating method. First, the stainless steel meshes were immersed in the polymer solutions and then drawn horizontally. Then, the polymer coated meshes were heated in an oven at 85°C for 180 min. For the sake of removing the nonreactive monomers, the polymer-coated meshes would be flushed by deionized water after polymerization. Consequently, the oil–water separation meshes were prepared and their oil–water separation efficiencies and antibacterial property would be examined.

2.6. Oil–water separation and durability test

In order to set up the filtration system, the oil–water separation mesh was welded between two stainless steel tubes with 50 mm of inner diameter. For preventing the leakage of oil–water mixtures (30 wt.%), the mesh was also sealed by using an O-ring and a clamp. After fixing the mesh, the oil–water mixtures were poured gently into the filtration system and the effluent was collected in a beaker. Since there is no external pressure applied to drive the liquid through the mesh, it would be said that the gravity-driven mesh filtration system was realized, as shown in Fig. 1. Then, the mass of effluent was measured in several sampling intervals and the permeate flux was calculated. Since the composition of collect effluent was water, the separation efficiency could be calculated by using oil rejection coefficient R (%) [42]:

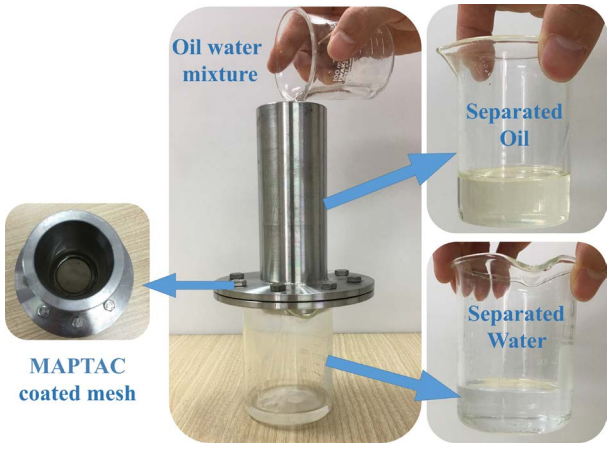

Fig. 1. Separation process of an oil-water mixture using MAPTAC coated mesh as a filter.

$$R(\%) = \left(1 - \frac{C_p}{C_0}\right) \times 100\% \quad (3)$$

where C_0 and C_p are the oil concentration of the original oil–water mixture and the oil concentration of the collected water after p times of the separation process, respectively. For the durability test, the same separation process was repeated 120 times for the same polymer-coated mesh.

2.7. Antibacterial test

The antimicrobial activity was assessed referring to the standard shake flask method (ASTM-E2149-01) [43–47], which could determine the antimicrobial activity. This method provides quantitative data for measuring the reduction rate in a number of colonies formed, converted to the average colony forming units per milliliter of buffer solution in the flask (CFU/mL). *E. coli* (ATCC 23815) was used as a model bacterium because of its wide reproduction in water. In the beginning, the target *E. coli* was cultured in Luria–Bertani (LB) broth at 37°C for 24 h to reach mid-log phase, and then the bacterial suspension was diluted with a 0.9% solution of NaCl at pH 6.5 to the cell concentration of 10^6–10^7 CFU/mL. Then, 5 mL of diluted solution was withdrawn and incubated with immersing a piece of polymer mesh (5 mm × 20 mm) within a test tube at 37°C. In order to determine the inoculum cell density, the suspensions were withdrawn before contacting with the polymer mesh and after contacting in 1 h. The withdrawn suspensions were diluted serially in the sterile buffer solution, spread on a nutrient plate count agar (PCA), and further incubated at 37°C for 24 h to determine the number of surviving bacteria. The colonies were counted and the antibacterial rate (AR) was defined as follows:

$$\mathrm{AR} = \left(\frac{n_0 - n}{n_0}\right) \times 100\% \quad (4)$$

where n_0 and n are the average number of bacteria before and after the contact with the dilute samples, respectively. All experiments were conducted in triplicate with data being only considered if the error between measurements was smaller than 15%.

2.8. Other characterizations

In order to understand the hydrophobicity of polymer-coated meshes, contact angles and surface tension were measured by using a contact angle meter (GBX-PX610, Germany). During the measurement, chloroform droplets (2 μL) were dropped carefully on the oil–water separation mesh underwater at ambient temperature. The average contact angle was determined by measuring more than five different positions on the same sample. The images of the polymer-coated meshes before and after filtration were obtained from a scanning electron microscope (SEM;

JEOL-I6700, Japan) with an acceleration voltage of 15 kV and the magnitude of 2,000X.

2.9. Chemical and thermal stability test

The oil–water separation tests of polymer-coated meshes under various severe circumstances were examined to determine the oil–water separation efficiency and chemical stability. The testing circumstances included acidic (1 M HCl), alkaline (1 M NaOH), and salty (8 wt.% NaCl) conditions. Besides, we also conducted the filtration test under high temperature of 80°C to verify its separation efficiency and thermal stability [28].

3. Results and discussion

3.1. Physical properties of polymers

Two kinds of quaternary ammonium monomers, MAETAC and MAPTAC, were used to synthesize the polymers and the schematic diagram of the polymerization reaction is represented in Fig. 2. It showed that polymers with different monomers of MAETAC and MAPTAC were both obtained successfully through the thermal polymerization with crosslinking agent, MBA. In addition, the conversion of the monomers exceeded 99% to form a polymer, indicated by the results of the potassium permanganate titration test.

The service life and stability of the polymers could be relative to their chemical structures, so hydrolysis resistance tests of these polymers were conducted. Since the end carboxyl-group concentration was derived from the hydrolysis of polymer, higher carboxyl group concentration indicated the higher degrees of hydrolysis. In this study, two kinds of polymers synthesized by MAETAC and MAPTAC noted as TE-1 and PT-1, respectively, were examined. Fig. 3 depicts the effect of hydrolysis time on the carboxyl group concentration of TE-1 and PT-1. The results revealed that the carboxyl group concentration of TE-1 increased with the hydrolysis time. When the hydrolysis time was 65 h, the carboxyl group concentration of TE-1 reached 64.7 mmol g^{-1}, indicating that TE-1 was easily hydrolyzed and not stable as a material for oil–water separation meshes [48–50]. On the contrary, the degree of hydrolysis of PT-1 increased by only 0.2 mmol g^{-1} after 65 h, implying that the hydrolysis

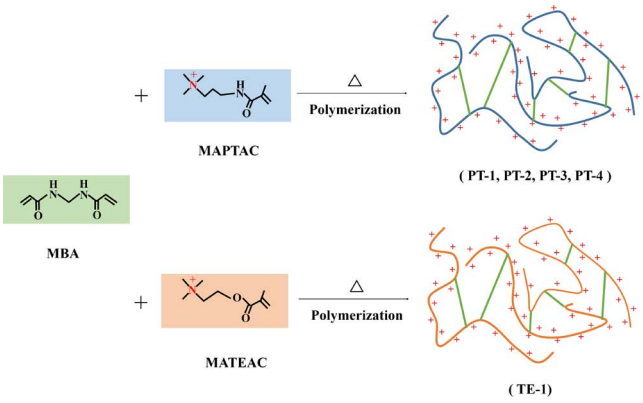

Fig. 2. Schematic diagram of the polymerization reaction.

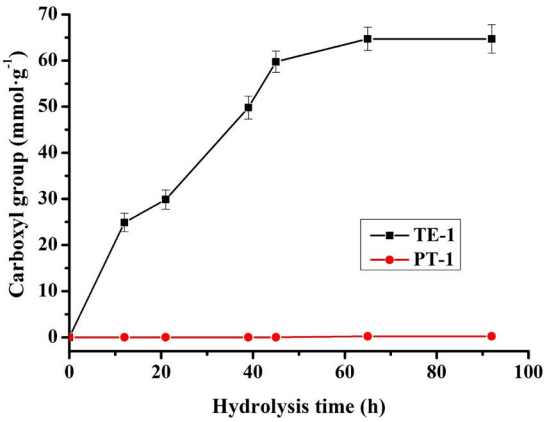

Fig. 3. Effect of different hydrolysis time on the carboxyl group concentration of TE-1 and PT-1.

resistance of PT-1 was superior to that of TE-1. Thus it could be concluded that PT-1 could be suitable for the application of oil–water separation.

Fig. 4 illustrates the effects of time on the swelling ratio of PT-1, PT-2, PT-3, and PT-4 which contained different proportions of the crosslinking agent. The swelling ratio of all the four polymers increased with time. In the first 10 min, the swelling ratio of the four polymers increased considerably. After 60 min, the swelling ratio for PT-1, PT-2, PT-3, and PT-4 became moderate and approached equilibrium. When the swelling time was 1,440 min, the swelling ratios were 29.7, 9.7, 7.2, and 5.7 g/g for PT-1, PT-2, PT-3, and PT-4, respectively. It showed that the swelling ratio at equilibrium decreased with increasing proportions of the crosslinking agent in the polymers. The main reason is that more proportions of crosslinking agent adding into the polymers resulted in higher degrees of crosslinking, which would limit free volumes of polymers and decrease the equilibrium swelling ratio.

3.2. Separation performance of the polymer coated meshes

The PT-1 polymer was deposited on various stainless steel meshes, which had a different pore size (4–150 μm). Then the prepared polymer-coated meshes were fabricated into the filtering system to verify the oil–water separation

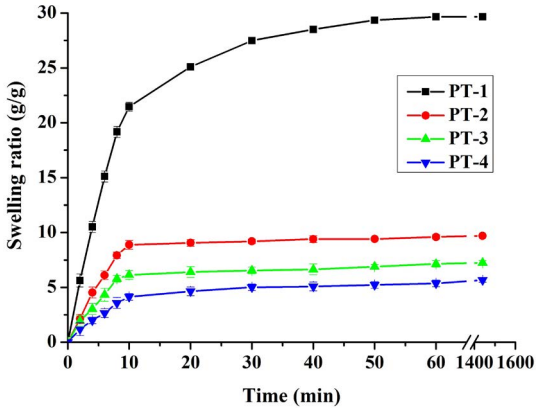

Fig. 4. Effect of different swelling time on swelling degrees of the polymers, such as PT-1, PT-2, PT-3, and PT-4.

efficiency and the permeate flux across the meshes. The separation efficiency and permeate flux of these polymer-coated meshes are shown in Fig. 5. It was revealed that increasing the mesh pores size resulted in decreasing separation efficiency and increasing permeate flux. In order to meet the requirement of high separation efficiency above 99%, the pore size of stainless steel should be lower than 45 μm. However, the permeate flux across the PT-1 coated meshes decreased from 4,308 to 470 L h^{-1} m^{-2} as the pore size decreased from 45 to 4 μm, indicating that 45 μm was the optimal mesh pore size.

Since the optimal mesh pore size was confirmed, various polymer-coated meshes by adding different amounts of crosslinking agent were synthesized and characterized. The oil–water separation efficiency and permeate flux of PT-1, PT-2, PT-3, and PT-4 are shown in Fig. 6. The results revealed that the separation efficiencies of PT-1, PT-2, PT-3, and PT-4 were 99.8%, 99.7%, 99.5%, and 99.4%, respectively. All of the separation efficiencies for these four types of meshes exceeded 99%. However, the permeate fluxes were 4,308; 4,848; 5,967; and 7,009 L h^{-1} m^{-2}, respectively, by using PT-1, PT-2, PT-3, and PT-4 mesh. The possible reason is that the swelling ratio of the polymers decreased with the increasing proportions of crosslinking agent, resulting in the larger pore size of the mesh. The higher pore size of the mesh allowed higher permeate flux across the mesh. Besides, the water contact angle and underwater oil contact angle of PT-1 mesh were 0° and 149°, respectively. It represented that PT-1 mesh was characterized as an oil-removal type separation mesh as well as PT-2, PT-3, and PT-4 showing the similar surface wettability. Besides vegetable oil, we also attempt to exploit the mixture of an organic solvent and water to examine the separation efficiency of the PT-1 mesh. The results showed that the prepared mesh could separate water from each mixture of toluene, heptane, diesel, or kerosene, with extremely high separation efficiencies of >99%, representing its good applicability for various organic-water mixtures.

3.3. Surface morphology, antibacterial property and durability of the polymer-coated meshes

Fig. 7a is the SEM image of the prepared PT-1 coated mesh for the oil–water separation. It could be observed that the surface of the mesh had the texture with some irregular lines. Compared with Fig. 7a, the SEM image of the PT-1 coated mesh after antibacterial test of *E. coli* suspension reveals some black spots on the fibers of the mesh as shown in Fig. 7b. The shape of these black spots is similar to that of *E. coli* described in the previous study [51,52]. In the

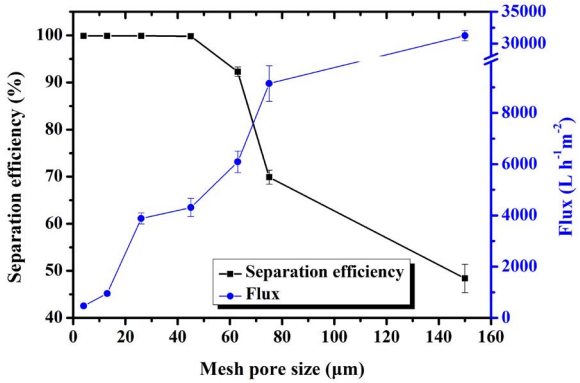

Fig. 5. The relationship of separation efficiency and permeate flux across the oil-water separation meshes (PT-1) with the variation of pore sizes of stainless steel meshes.

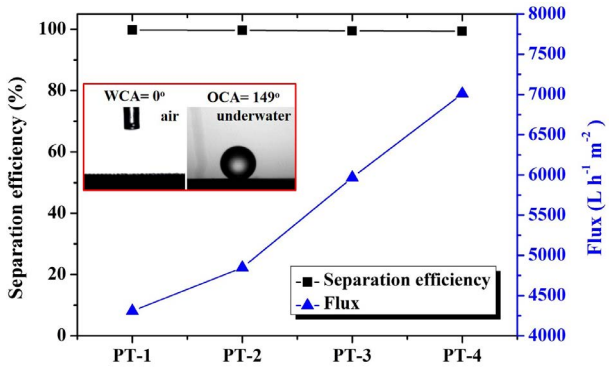

Fig. 6. Separation efficiency and permeate flux of PT-1, PT-2, PT-3, and PT-4 oil-water separation meshes. The photograph showed that the water contact angle (WCA) and underwater oil contact angle (OCA) of PT-1 mesh.

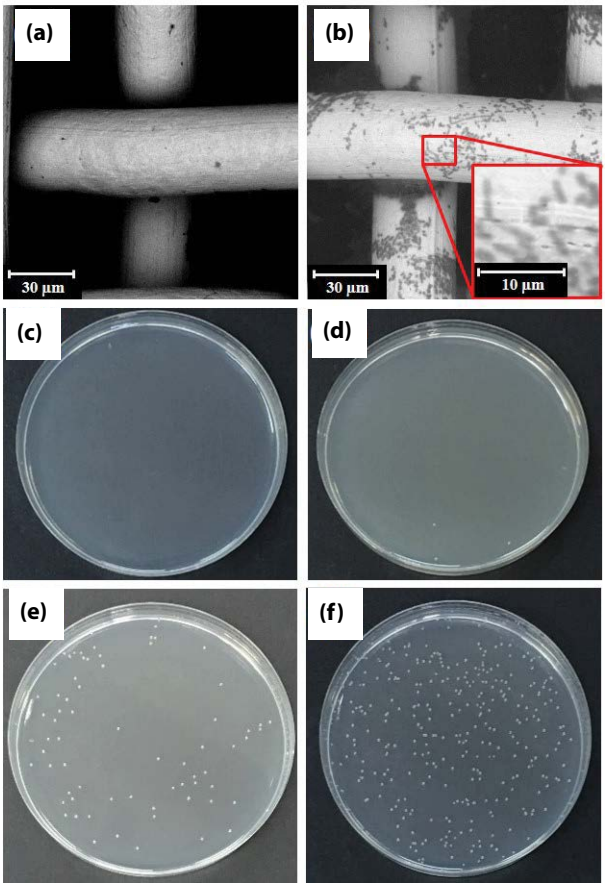

Fig. 7. (a) The SEM image of the PT-1 mesh at the initial state, (b) the SEM image of the PT-1 mesh after the antibacterial test. The pictures of plate counting results after antibacterial test of (c) PT-1, (d) PT-2, (e) PT-3, and (f) PT-4 meshes.

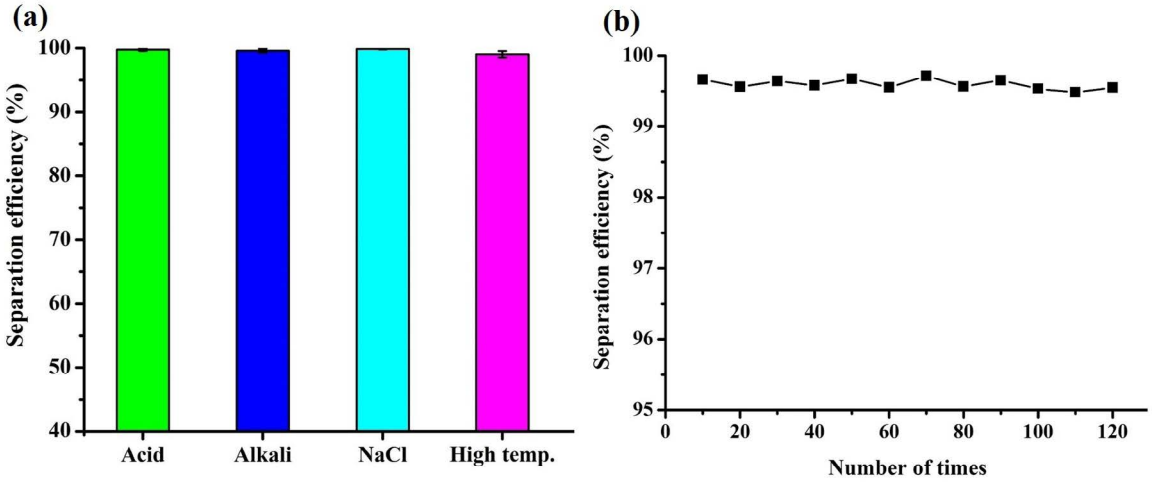

Fig. 8. (a)Effect of oil-water mixtures in different conditions on oil-water separation efficiency by using a PT-1 oil-water separation mesh and (b) The durability test for the PT-1 oil-water separation mesh.

antibacterial test, the negative charges of *E. coli* easily attract the positive surface charge of poly-quaternary ammonium salt mesh; thus the *E. coli* are easily adsorbed onto the prepared mesh. Sequentially, the internal charge balance of the *E. coli's* cell wall would be destroyed, leading to the death of *E. coli* [36,53]. For the antibacterial test, Figs. 7c–f show the pictures of incubated PCAs which were spread on the diluted eluent after filtering process by using PT-1, PT-2, PT-3, and PT-4 meshes. The stainless steel meshes without coated polymer were also examined as the control experiment, and it showed no antibacterial property through the plate counting method. On contrary, the antibacterial property of PT-1, PT-2, PT-3, and PT-4 meshes could be calculated as above 99.99%, 99.99%, 99.93%, and 99.67%, respectively. To sum up, as the proportion of crosslinking agent increased, the density of the quaternary ammonium molecule would be lower, thereby resulting in a decrease of the antibacterial property [36].

Fig. 8a shows that the oil–water separation efficiencies of the PT-1 polymer-coated mesh were not affected under various severe conditions, such as acidic (1 M HCl), alkaline (1 M NaOH), and salty (8 wt.% NaCl) solution. Their oil–water separation efficiencies were kept above 99%. In addition, it also proved that the oil–water separation efficiency could reach more than 99% even under the operation at a high temperature up to 80°C. The above results showed that the PT-1 polymer-coated mesh had a wide range of operating condition for separating the oil–water mixture.

Consequently, the durability of the PT-1 polymer-coated mesh was also verified as shown in Fig. 8b. The oil–water separation efficiencies could be maintained above 99.5% even repeating 120 times of oil–water separation procedures. It indicated that PT-1 polymer-coated mesh was not only facile but also stable for the potential in practical utilization.

4. Conclusions

In this study, polymer-coated meshes were demonstrated for the filtration of oil–water separation. The optimal polymer-coated meshes were fabricated by the stainless steel meshes coated with the PT-1 polymer. From the result of hydrolysis resistance test under soaking in 0.5 M hydrochloric acid solution, the carboxyl group of the polymers composed of MAPTAC and MAETAC were identified as 0.2 and 64.7 mmol g^{-1}, respectively. It indicates that the MAPTAC polymer provided better resistance against the hydrolysis reaction. Besides, the swelling ratio of the MAPTAC polymers was also investigated. It shows that higher amount of crosslinking agent caused the limitation of free volumes of polymers, resulting in the reduction of swelling ratio. For the MAPTAC polymers, an optimal stainless steel mesh with a pore size of 45 μm was identified with due consideration of its good oil–water separation efficiency and high permeate flux. The MAPTAC polymer-coated meshes exhibited excellent oil–water separation efficiency above 99% with high permeate flux, varied in the range of 4,308–7,009 L h^{-1} m^{-2}. Moreover, their antibacterial properties against *E. coli* were verified by the result of the antibacterial test. The few numbers of colonies per plate originated from the diluted eluent revealed that PT-1 coated mesh had good antibacterial property. Furthermore, this polymer-coated mesh also displayed favorable resistance and good oil–water separation efficiency (>99%) under the severe chemical circumstances, including acidic (1 M HCl), alkaline (1 M NaOH), and salty (8 wt.% NaCl) conditions. It also performed high oil–water separation efficiency under the operation at a high temperature of 80°C. Most importantly, the durability (up to 120 times) with similar separation efficiency (>99%) suggests that the polymer-coated mesh exhibits a strong potential for the practical treatment of oil–water separation in the near future.

References

[1] M.A. Shannon, P.W. Bohn, M. Elimelech, J.G. Georgiadis, B.J. Marinas, A.M. Mayes, Science and technology for water purification in the coming decades, Nature, 452 (2008) 301–310.
[2] J. Yuan, X. Liu, O. Akbulut, J. Hu, S.L. Suib, J. Kong, F. Stellacci, Superwetting nanowire membranes for selective absorption, Nat. Nanotechnol., 3 (2008) 332–336.
[3] W. Chung, S. Young, Evaluation of a chemical dissolved air flotation system for the treatment of restaurant dishwasher effluent, Can. J. Civ. Eng., 40 (2013) 1164–1172.

[4] M. Ji, X.G. Jiang, F. Wang, A mechanistic approach and response surface optimization of the removal of oil and grease from restaurant wastewater by electrocoagulation and electroflotation, Desal. Wat. Treat., 55 (2015) 2044–2052.
[5] G. Chen, Electrochemical technologies in wastewater treatment, Sep. Purif. Technol., 38 (2004) 11–41.
[6] J.S. Eow, M. Ghadiri, Electrostatic enhancement of coalescence of water droplets in oil: a review of the technology, Chem. Eng. J., 85 (2002) 357–368.
[7] M. Hanafy, H.I. Nabih, Treatment of oily wastewater using dissolved air flotation technique, Energy Sources Part A, 29 (2007) 143–159.
[8] W.-T. Kwon, K. Park, S.D. Han, S.M. Yoon, J.Y. Kim, W. Bae, Y.W. Rhee, Investigation of water separation from water-in-oil emulsion using electric field, J. Ind. Eng. Chem., 16 (2010) 684–687.
[9] Y. Suzuki, T. Maruyama, Removal of emulsified oil from water by coagulation and foam separation, Sep. Sci. Technol., 40 (2005) 3407–3418.
[10] J.J. Lee, Y.C. Woo, J.-S. Kang, C.Y. Kang, H.-S. Kim, Effect of various pretreatments on the performance of nanofiltration for wastewater reuse, Desal. Wat. Treat., 57 (2016) 7522–7530.
[11] B. Ge, X. Men, Y. Li, Z. Zhang, One-step foaming method to functional polyurethane absorbents foam, Sep. Sci. Technol., 51 (2016) 1299–1306.
[12] N. Derlon, N. Koch, B. Eugster, T. Posch, J. Pernthaler, W. Pronk, E. Morgenroth, Activity of metazoa governs biofilm structure formation and enhances permeate flux during Gravity-Driven Membrane (GDM) filtration, Water Res., 47 (2013) 2085–2095.
[13] X. Tang, Y. Si, J. Ge, B. Ding, L. Liu, G. Zheng, W. Luo, J. Yu, In situ polymerized superhydrophobic and superoleophilic nanofibrous membranes for gravity driven oil–water separation, Nanoscale, 5 (2013) 11657–11664.
[14] T. Yan, H.W. Meng, W.J.H. Hu, F.P. Jiao, Superhydrophilicity and underwater superoleophobicity graphene oxide-micro crystalline cellulose complex-based mesh applied for efficient oil/water separation, Desal. Wat. Treat., 111 (2018) 155–164.
[15] Y. Feng, Z. Wang, R. Zhang, Y. Lu, Y. Huang, H. Shen, X. Lv, J. Liu, Anti-fouling graphene oxide based nanocomposites membrane for oil-water emulsion separation, Water Sci. Technol., 77 (2018) 1179–1185.
[16] M. Liu, S. Wang, Z. Wei, Y. Song, L. Jiang, Bioinspired design of a superoleophobic and low adhesive water/solid interface, Adv. Mater., 21 (2009) 665–669.
[17] Y.-Q. Liu, Y.-L. Zhang, X.-Y. Fu, H.-B. Sun, Bioinspired underwater superoleophobic membrane based on a graphene oxide coated wire mesh for efficient oil/water separation, ACS Appl. Mater. Interfaces, 7 (2015) 20930–20936.
[18] X.Y. Zhang, C.Q. Wang, X.Y. Liu, J.H. Wang, C.Y. Zhang, Y.L. Wen, PVA/SiO_2-coated stainless steel mesh with superhydrophilic-underwater superoleophobic for efficient oil-water separation, Desal. Wat. Treat., 126 (2018) 157–163.
[19] C. Marconnet, A. Houari, D. Seyer, M. Djafer, G. Coriton, V. Heim, P. Di Martino, Membrane biofouling control by UV irradiation, Desalination, 276 (2011) 75–81.
[20] J. Wang, X. Gao, Q. Wang, H. Sun, X. Wang, C. Gao, Enhanced biofouling resistance of polyethersulfone membrane surface modified with capsaicin derivative and itaconic acid, Appl. Surf. Sci., 356 (2015) 467–474.
[21] Y. Wu, X. Zhang, S. Liu, B. Zhang, Y. Lu, T. Wang, Preparation and applications of microfiltration carbon membranes for the purification of oily wastewater, Sep. Sci. Technol., 51 (2016) 1872–1880.
[22] M. Bojarska, W. Piatkiewicz, Antibacterial properties of membranes modified by acrylic acid with silver nanoparticles, Desal. Wat. Treat., 56 (2015) 3196–3202.
[23] H. Li, D.B. Cheng, L.Y. Dong, F. Qian, Enhancement in permselectivity and antibacterial performances of polyamide RO membranes via surface modification of AgCl nanoparticles, Desal. Wat. Treat., 116 (2018) 19–28.
[24] H.-C. Flemming, Biofilms and Environmental protection, Water Sci. Technol., 27 (1993) 1–10.
[25] M. Herzberg, M. Elimelech, Biofouling of reverse osmosis membranes: role of biofilm-enhanced osmotic pressure, J. Membr. Sci., 295 (2007) 11–20.
[26] H.-C. Flemming, G. Schaule, T. Griebe, J. Schmitt, A. Tamachkiarowa, Biofouling—the Achilles heel of membrane processes, Desalination, 113 (1997) 215–225.
[27] N. Misdan, A.F. Ismail, N. Hilal, Recent advances in the development of (bio)fouling resistant thin film composite membranes for desalination, Desalination, 380 (2016) 105–111.
[28] J. Liu, W. He, P. Li, S. Xia, X. Lu, Z. Liu, P. Yan, T. Tian, Synthesis of graphene oxide-SiO_2 coated mesh film and its properties on oil-water separation and antibacterial activity, Water Sci. Technol., 73 (2016) 1098–1103.
[29] R.K. Upadhyay, A. Dubey, P.R. Waghmare, R. Priyadarshini, S.S. Roy, Multifunctional reduced graphene oxide coated cloths for oil/water separation and antibacterial application, RSC Adv., 6 (2016) 62760–62767.
[30] T. Suryaprabha, M.G. Sethuraman, Fabrication of copper-based superhydrophobic self-cleaning antibacterial coating over cotton fabric, Cellulose, 24 (2016) 395–407.
[31] P. Gilbert, L.E. Moore, Cationic antiseptics: diversity of action under a common epithet, J. Appl. Microbiol., 99 (2005) 703–715.
[32] W. Sajomsang, S. Tantayanon, V. Tangpasuthadol, W.H. Daly, Quaternization of N-aryl chitosan derivatives: synthesis, characterization, and antibacterial activity, Carbohydr. Res., 344 (2009) 2502–2511.
[33] H. Yu, X. Zhang, Y. Zhang, J. Liu, H. Zhang, Development of a hydrophilic PES ultrafiltration membrane containing SiO_2@N-Halamine nanoparticles with both organic antifouling and antibacterial properties, Desalination, 326 (2013) 69–76.
[34] J.H. Kim, D.C. Choi, K.M. Yeon, S.R. Kim, C.H. Lee, Enzyme-immobilized nanofiltration membrane to mitigate biofouling based on quorum quenching, Environ. Sci. Technol., 45 (2011) 1601–1607.
[35] D. Alves, M. Olivia Pereira, Mini-review: antimicrobial peptides and enzymes as promising candidates to functionalize biomaterial surfaces, Biofouling, 30 (2014) 483–499.
[36] H. Murata, R.R. Koepsel, K. Matyjaszewski, A.J. Russell, Permanent, non-leaching antibacterial surface—2: how high density cationic surfaces kill bacterial cells, Biomaterials, 28 (2007) 4870–4879.
[37] B. Simoncic, B. Tomsic, Structures of novel antimicrobial agents for textiles - a review, Text. Res. J., 80 (2010) 1721–1737.
[38] C. Yao, X. Li, K.G. Neoh, Z. Shi, E.T. Kang, Surface modification and antibacterial activity of electrospun polyurethane fibrous membranes with quaternary ammonium moieties, J. Membr. Sci., 320 (2008) 259–267.
[39] C. Yao, X.-S. Li, K.G. Neoh, Z.-l. Shi, E.T. Kang, Antibacterial poly(D,L-lactide) (PDLLA) fibrous membranes modified with quaternary ammonium moieties, Chinese J. Polym. Sci., 28 (2010) 581–588.
[40] Q.H. Feng, Q.H. Tang, W.L. Zhang, Y.H. Jia, D. Zhang, End-group method for molecular weight determination of PET depolymerization under microwave irradiation, Adv. Mat. Res., 554–556 (2012) 1933–1937.
[41] X. Qi, M. Liu, Z. Chen, F. Zhang, Study on the swelling kinetics of superabsorbent using open circuit potential measurement, Eur. Polym. J., 44 (2008) 743–754.
[42] Z. Xue, S. Wang, L. Lin, L. Chen, M. Liu, L. Feng, L. Jiang, A novel superhydrophilic and underwater superoleophobic hydrogel-coated mesh for oil/water separation, Adv. Mater., 23 (2011) 4270–4273.
[43] T.P. Martin, S.E. Kooi, S.H. Chang, K.L. Sedransk, K.K. Gleason, Initiated chemical vapor deposition of antimicrobial polymer coatings, Biomaterials, 28 (2007) 909–915.
[44] X. Liu, T. Lin, B.X. Peng, X.G. Wang, Antibacterial activity of capsaicin-coated wool fabric, Text. Res. J., 82 (2012) 584–590.
[45] L.F. Zemljic, T. Tkavc, A. Vesel, O. Sauperl, Chitosan coatings onto polyethylene terephthalate for the development of potential active packaging material, Appl. Surf. Sci., 265 (2013) 697–703.
[46] D. Coelho, A. Sampaio, C. Silva, H.P. Felgueiras, M.T.P. Amorim, A. Zille, Antibacterial electrospun poly (vinyl alcohol)/ enzymatic synthesized poly(catechol) nanofibrous midlayer

membrane for ultrafiltration, ACS Appl. Mater. Interfaces, 9 (2017) 33107–33118.
[47] H.X. Yu, Y.T. Zhang, J.Y. Zhang, H.Q. Zhang, J.D. Liu, Preparation and antibacterial property of SiO_2-Ag/PES hybrid ultrafiltration membranes, Desal. Wat. Treat., 51 (2013) 3584–3590.
[48] P. van de Wetering, N.J. Zuidam, M.J. van Steenbergen, O.A.G.J. van der Houwen, W.J.M. Underberg, W.E. Hennink, A mechanistic study of the hydrolytic stability of poly(2-(dimethylamino) ethyl methacrylate), Macromolecules, 31 (1998) 8063–8068.
[49] A.M. Funhoff, C.F. van Nostrum, A.P.C.A. Janssen, M.H.A.M. Fens, D.J.A. Crommelin, W.E. Hennink, Polymer side-chain degradation as a tool to control the destabilization of polyplexes, Pharm. Res., 21 (2004) 170–176.
[50] M. Vetrík, M. Přádný, M. Hrubý, J. Michálek, Hydrazone-based hydrogel hydrolytically degradable in acidic environment, Polym. Degrad. Stabil., 96 (2011) 756–759.
[51] W.Y. Wang, L.Y. Zhu, B.J. Shan, C.C. Xie, C.N. Liu, F.Y. Cui, G.F. Li, Preparation and characterization of SLS-CNT/PES ultrafiltration membrane with antifouling and antibacterial properties, J. Membr. Sci., 548 (2018) 459–469.
[52] J.C. Gu, P. Xiao, L. Zhang, W. Lu, G.G. Zhang, Y.J. Huang, J.W. Zhang, T. Chen, Construction of superhydrophilic and under-water superoleophobic carbon-based membranes for water purification, RSC Adv., 6 (2016) 73399–73403.
[53] R. Kugler, O. Bouloussa, F. Rondelez, Evidence of a charge-density threshold for optimum efficiency of biocidal cationic surfaces, Microbiology, 151 (2005) 1341–1348.